Epithelial membrane protein 3 regulates lung cancer stem cells via the TGF-β signaling pathway

YEON-JEE KAHM[1,2*], RAE-KWON KIM[1,2*], UHEE JUNG[1] and IN-GYU KIM[1,2]

[1]Department of Radiation Biology, Environmental Safety Assessment Research Division, Korea Atomic Energy Research Institute, Daejeon 34057; [2]Department of Radiation Science and Technology, Korea University of Science and Technology, Daejeon 34113, Republic of Korea

Received May 25, 2021; Accepted August 9, 2021

DOI: 10.3892/ijo.2021.5261

Abstract. Epithelial membrane protein 3 (EMP3) is a transmembrane glycoprotein that contains a peripheral myelin protein 22 domain. EMP3 first received attention as a tumor suppressor, but accumulating evidence has since suggested that it may exhibit a tumor-promoting function. Nonetheless, the biological function of EMP3 remains largely unclear with regards to its role in cancer. Herein, it was shown that EMP3 expression is upregulated in non-small cell lung cancer (NSCLC) cells overexpressing aldehyde dehydrogenase 1 (ALDH1). EMP3 was shown to be involved in cell proliferation, the formation of cancer stem cells (CSCs) and in epithelial-mesenchymal transition (EMT). The ability to resist irradiation, one of the characteristics of CSCs, decreased when the EMP3 mRNA expression was knocked down using small interfering RNA. In addition, when EMP3 knockdown reduced the migratory ability of cells, a characteristic of EMT. Additionally, it was shown that the TGF-β/Smad signaling axis was a target of EMP3. EMP3 was found to interact with TGF-β receptor type 2 (TGFBR2) upon TGF-β stimulation in lung CSCs (LCSC). As a result, binding of EMP3-TGFBR2 regulates TGF-β/Smad signaling activation and consequently affects CSCs and EMT. Kaplan-Meier analysis results confirmed that patients with high expression of EMP3 had poor survival rates. Taken together, these findings showed that EMP3 may be a potential target for management of LCSCs with high expression of ALDH1, and that EMP3 is involved in TGF-β/Smad signaling activation where it promotes acquisition of cancerous properties in tumors.

Correspondence to: Dr In-Gyu Kim, Department of Radiation Biology, Environmental Safety Assessment Research Division, Korea Atomic Energy Research Institute, 111 Daedeok-Daero 989 Beon-Gil, Yuseong-Gu, Daejeon 34057, Republic of Korea
E-mail: igkim@kaeri.re.kr

*Contributed equally

Key words: epithelial membrane protein 3, aldehyde dehydrogenase 1, lung cancer stem cells, TGF-β signaling, epithelial-mesenchymal transition

Introduction

The epithelial membrane protein 3 (EMP3), a member of the peripheral myelin protein 22-kDa (PMP22) gene family, is a small hydrophobic membrane glycoprotein, and a myelin-related gene. The protein encoded by this gene contains two N-linked glycosylation sites and four transmembrane domains (1). In several studies, EMP3 has been reported to function as a tumor suppressor gene in solid tumors (2-4). However, EMP3 has also been shown to function as an oncogene in several other malignancies, particularly brain tumors, breast carcinoma and hepatocellular carcinoma (5-7). Primary glioblastoma multiforme (GBM) frequently exhibits upregulated expression of EMP3 (5). In addition, EMP3 mRNA upregulation may be a suitable molecular marker to predict clinical outcomes in patients with GBM (8). Taken together, these studies suggest that EMP3 is an important gene that promotes tumorigenesis in primary GBM. However, the molecular mechanism of EMP3 in non-small cell lung cancer (NSCLC) has not been studied previously, to the best of our knowledge, and thus requires investigation.

Worldwide, lung cancer has a poor prognosis for both men and women. NSCLC accounts for the majority (≥75%) of lung cancer cases, and is the leading cause of cancer-related death worldwide (9,10). Despite the use of conventional chemotherapy and radiation therapy, NSCLC cannot be effectively treated, and lung injury may occur as a side effect of these treatments (11). Although various studies have been performed on cell proliferation, invasion and migration of NSCLC, the mechanism underlying the development of NSCLC in the first place is unclear, and the 5-year survival rate of patients with NSCLC is <15%. Metastasis is the cause of death in >90% of patients with solid tumors, including in patients with NSCLC (12), and cancer stem cells (CSCs) are involved in recurrence and in metastasis (13). CSCs are involved in tumor initiation, growth and maintenance and are also called tumor initiating cells (14). CSCs exhibit the self-renewal ability of normal stem cells, can differentiate into cells of various phenotypes, and are resistant to radiation or chemotherapy (15,16). CSCs can be identified using specific marker

proteins for each tissue. In the case of lung cancer, cancer stem cells can be selected by CD133, CD44 and ALDH (17,18). In particular, ALDH is used as a marker protein in cancer stem cells of various tissues, including breast cancer, brain cancer, and colorectal cancer, in addition to lung cancer (19-21).

Lung CSCs (LCSCs) are becoming an increasingly studied target for treatment of lung cancer (22). Accordingly, several pharmaceutical companies are attempting to develop anticancer drugs targeting CSCs specifically, and several drugs are being used in patients (23-25). Various tumors, including LCSCs, affect the malignancy and clinical prognosis by activation of the TGF-β signaling pathway (26,27). The activation of TGF-β signaling enhances the ability of cells to migrate and promote the epithelial-mesenchymal transition (EMT), which is associated with metastasis (28,29). Cell motility is important for metastasis from the primary site to the secondary site via lymph or blood vessels (30,31). In the present study, it was shown for the first time that EMP3 is involved in maintaining the characteristics of LCSCs via direct binding to TGFBR2.

Materials and methods

Cell culture and sphere-formation assays. Human A549 and H460 lung cancer cell lines were purchased from the Korea Cell Line Bank and grown using RPMI-1640 medium (cat. no. SH30027.01; HyClone; Cytiva) supplemented with 10% (v/v) FBS (cat. no. SH30919.03; HyClone; Cytiva), 1% streptomycin and 1% penicillin (cat. no. SV30010; HyClone; Cytiva). Cells were cultured in a humidified incubator with 5% CO_2 at 37˚C. During the sphere formation assay, cells were cultured in stem cell-acceptable DMEM (DMEM-F12; cat. no. 11320-033; Invitrogen; Thermo Fisher Scientific, Inc.) supplemented with basic fibroblast growth factor (bFGF; 20 ng/ml; cat. no. 13256-029; Invitrogen; Thermo Fisher Scientific, Inc.), epidermal growth factor (20 ng/ml; cat. no E9644; Sigma-Aldrich; Merck KGaA) and B27 Serum-Free Supplement (cat. no. 17504-044; Invitrogen; Thermo Fisher Scientific, Inc.). Single cell experiments were set up with floating cells in an ultra-low adhesion 96-well plate (cat. no. 3474; Corning, Inc.) with 1 or 2 cells distributed per well. The cells were cultured in a humidified incubator as above. The following day, only wells with single cells in each well were selected visually under a light microscope (magnification, x400), and after 10-14 days, spheres were quantified based on absolute count as well as diameter, and photographed using an inverted phase contrast microscope.

Sorting CSCs from A549 cells. An ALDEFLUOR™ assay (cat. no. 01700; Stemcell Technologies, Inc.) was used to isolate the CSC population from A549 cells according to the manufacturer's protocol. A total of $1x10^6$ cells were harvested and resuspended in ALDEFLUOR assay buffer containing ALDH substrate. As a negative control, an aliquot of cells exposed to ALDEFLUOR was immediately quenched with the specific ALDH inhibitor N,N-diethylaminobenzaldehyde. After 30 min of incubation at 37˚C, cells were washed and sorted into ALDH1high and ALDH1low cells using a FACSAria flow cytometer (BD Biosciences), and analyzed using BD FACSDiva version 6.1.3 (BD Biosciences).

DNA microarray for gene expression profiling. The quality of total RNA was measured using Agilent's 2100 Bioanalyzer System (Agilent Technologies, Inc.). Amplification and labeling were performed using the Low RNA Input Linear Amplification kit PLUS (cat. no. 5185-5818; Agilent Technologies, Inc.). Microarray hybridization was performed using the Gene Expression Hybridization kit (cat. no. 5188-5242; Agilent Technologies, Inc.). Microarray washes were performed using the Gene Expression Wash Buffer kit (cat. no. 5190-0448; Agilent). Finally, scanning and image analysis was performed using a DNA microarray scanner (cat. no. G4900DA; Agilent Technologies, Inc.) with the Feature Extraction Software (cat. no. G4460AA; Agilent Technologies, Inc.). All procedures were performed according to the manufacturer's protocol.

Small interfering RNA (siRNA) mediated knockdown of EMP3 and TGFBR2. A549 cells were transfected with siRNA targeting EMP3 or TGFBR2 (Bioneer Corporation) the sequences of which are listed in Table SI. 10 pmol siRNAs were transfected using Lipofectamine RNAi MAX reagent (cat. no. 13-778-150; Invitrogen; Thermo Fisher Scientific, Inc.). Stealth RNAi Negative Control Medium GC (cat. no. 12935-300; Invitrogen; Thermo Fisher Scientific, Inc.) was used as the negative control. Cells were incubated at 37˚C for 72 h after transfection.

DNA constructs. cDNA encoding full-length human EMP3 was generated by reverse transcription-PCR from total RNA extracted from A549 cells. RNA was extracted using TRIzol® (cat no. TR118; MRC). cDNA was synthesized from the extracted RNA using an RT PreMix at 60˚C for 1 h (cat no. 25264; Intron Biotechnology, Inc.). The sequences of the primers used for PCR were: RMP3 forward, TATAAGCTT ATGTCACTCCTCTTGCTGGTGG and reverse, ATATGA ATTCTCACTCCCGCTTCCGTAGG. For reverse transcription-PCR, PCR PreMix (cat no. 250256; Intron Biotechnology, Inc.) was used. The thermocycling conditions were; Initial denaturation at 94˚C for 30 sec; followed by 34 cycles of denaturation at 94˚C for 30 sec, annealing at 57.2˚C for 40 sec, and extension at 72˚C for 1 min. The results were confirmed using a 2% agarose gel (cat no. 161-3102; Bio-Rad Laboratories, Inc.). The cDNA was cloned into the mammalian expression vector pcDNA3.1 (Invitrogen; Thermo Fisher Scientific, Inc.).

Limiting dilution assay. Cells were plated in 100 μl spheroid formation assay medium in ultra-low adhesion 96-well plates. A total of 1, 10, 50, 100 or 200 cells/well were plated, with 48 wells for each starting density of cells. Analysis of oncospheres was performed using alight microscope (magnification, x400) after 12-20 days of incubation. A well with at least one spheroid with a diameter ≥100 μm was defined as a positive well, and the number of positive wells were counted.

Antibodies. Antibodies against EMP3 (cat. no. ab236671; Abcam), Sox2 (sex determining region Y-box 2; cat. no. 3579; Cell Signaling Technology, Inc.), phosphorylated (p)-Smad2 (cat. no. 18338; Cell Signaling Technology, Inc.), p-Smad3 (cat. no. 9520; Cell Signaling Technology, Inc.), Smad2/3 (cat. no. 5678; Cell Signaling Technology, Inc.), β-actin (cat. no. sc-7963;

Santa Cruz Biotechnology, Inc.), TGFBR1 (cat. no. sc-518086; Santa Cruz Biotechnology, Inc.), TGFBR2 (cat. no. sc-17791; Santa Cruz Biotechnology, Inc.), TGFBR3 (cat. no. sc-74511; Santa Cruz Biotechnology, Inc.), CD44 (cat. no. 5640; Cell Signaling Technology, Inc.), β-catenin (cat. no. sc-7963; Santa Cruz Biotechnology, Inc.), Twist (cat. no. sc-15393; Santa Cruz Biotechnology, Inc.), Vimentin (MA5-16409; Thermo Fisher Scientific, Inc.), aldehyde dehydrogenase (ALDH1)A1 (cat. no. ab52492; Abcam), ALDH1A3 (cat. no. ab129815; Abcam), Snail (cat. no. sc-10432; Santa Cruz Biotechnology, Inc.), Slug (cat. no. sc-166476; Santa Cruz Biotechnology, Inc.), ZEB1 (Zinc finger E-box-binding homeobox 1; cat. no. sc-25388; Santa Cruz Biotechnology, Inc.), E-cadherin (cat. no ab15148; Abcam), N-cadherin (cat. no. 610921; BD Biosciences) and Oct4 (cat. no. 2750; Cell Signaling Technology, Inc.) were used. Thsese antibodies were used for immunofluorescence assays, western blot analysis and/or immunoprecipitation (IP).

Neutralization assay. The anti-EMP3 antibody (1:100) was used for the neutralization assay. The normal mouse IgG1 antibody (cat. no. sc-3877; Santa Cruz Biotechnology, Inc.) was used as the control antibody. The experiment was conducted in the same manner as the cell culture environment, and the subsequent experiments or results were performed/obtained after 24-48 h.

TGF-β2 treatment. A total of 20 ng/ml TGFB3 (cat. no. 302-B2; Bio-Techne) was added to cells, and cells were cultured in an incubator for 24 h.

Western blotting and IP. Cells were mixed with lysis buffer [150 mM NaCl, 1 mM EDTA, 1 mM EGTA, 0.5% Triton X-100 in 20 mM Tris-HCl (pH 7.5)] and protease inhibitor cocktail (cat. no. P8340; Sigma-Aldrich; Merck KGaA). The protein concentration was measured using Bradford reagent (cat. no. 5000006, Bio-Rad Laboratories, Inc.) and normalized to a standard curve developed using known concentrations of BSA. For western blot analysis, 20 μg protein sample was loaded on 8-15% SDS-gels, resolved using SDS-PAGE and transferred to Hybond nitrocellulose membranes (cat. no. 10-6000-04; Amersham; Cytiva). Membranes were treated with specific antibodies all at a dilution of 1:1,000 overnight in a cold chamber at 4˚C. After washing with Tris-buffered saline (cat. no. TR2008-100-00; Biosesang), the membrane was treated with an horseradish peroxidase-conjugated secondary antibody (cat. no. anti-rabbit; cat. no. ab205718; or anti-mouse; cat. no. ab205719; both 1:10,000; Abcam) for 2 h at room temperature, and a Westzol enhanced chemiluminescence detection kit (cat. no. sc-2048; Santa Cruz Biotechnology, Inc.) was used to visualize signals.

IP was performed overnight at 4˚C using a concentration of 1:200 concentration-specific antibody (anti-EMP3; cat. no. ab236671; Abcam; or anti-TGFBR2; cat. no. sc-17791; Santa Cruz Biotechnology, Inc.) with 2 mg cell lysate. Then, 0.2 μg protein A/G Ultralink Resin (cat. no. sc-2003; Santa Cruz Biotechnology, Inc.) was added and incubated for 2 h at 4˚C. After washing with lysis buffer on the reacted samples, the immunoprecipitate was resuspended in 2x SDS sample buffer, and analyzed by western blotting using the specific antibodies (anti-EMP3 using the same antibody as above; and anti-TGFBR1; cat. no. sc-518086; anti-TGFBR2; cat. no. sc-17791; and anti-TGFBR3; cat. no. sc-74511; all from Santa Cruz Biotechnology, Inc.).

Invasion and migration assays. Migration assays were performed using an uncoated chamber (cat. no. 3422; 8-μm pore; Corning, Inc.) and the ability of cells to migrate was measured. Invasion assays were performed by coating the chamber with Matrigel® according to the manufacturer's protocol. The lower chamber of the Transwell inserts (Cell Biolabs) was filled with 800 μl RPMI-1640 supplemented with 10% FBS. In the upper chamber, 150 μl serum-free medium (Opti-MEM®; cat. no. 31985-070; Invitrogen; Thermo Fisher Scientific, Inc.) containing $2x10^5$ cells was added. The cells were incubated for 24 h at 37˚C in a humidified incubator with 5% CO_2. Cells that had migrated/invaded to the bottom of the chamber were stained with crystal violet (cat. no. HT90132-1L; Sigma-Aldrich; Merck KGaA) and the cells were counted under a light microscope (x400, magnification).

Wound healing assay. Cells were plated in a 60 mm culture dish and grown to 80% confluence. A wound was created by scraping the monolayer of cells with a 200 μl pipette tip in the middle. Floating cells were removed by washing with PBS and fresh medium containing 10% FBS was added. The doubling time of the A549 cells used was 22 h. Cells were incubated at 37˚C for 24 h, and imaged using phase-contrast microscopy (magnification, x400). The distance between the edges of the wounds shown in the image was measured randomly at three or more places and the mean of the three measurements were obtained.

Colony-formation assay and irradiation. Cells were seeded at a density of $1x10^3$ cells per 35-mm cell culture dish (cat. no. 430165; Corning, Inc.), and then allowed to adhere for 24 h in a humidified incubator with 5% CO_2 at 37˚C. The following day, cells were irradiated with 3 Gy γ-radiation (KAERI). After 10-14 days, cells were stained for colonies (defined as clusters of ≥50 cells) with 0.5% crystal violet for 1 h at room temperature, and stained colonies were counted. Clonal survival rates are expressed as a percentage of the non-irradiated control group.

Immunocytochemistry. In 6 well plates (cat. no. 3516; Corning, Inc.), $5x10^4$ cells were grown on glass coverslips and fixed with 4% paraformaldehyde (cat. no. P2031; Biosesang) for 1 h at room temperature. After fixing, cells were incubated overnight at 4˚C with antibodies in a solution of PBS containing 0.1% Triton X-100 (cat. no. 161-0781; Bio-Rad Laboratories, Inc.) and 1% BSA (cat. no. BSAS 0.1; Bovogen). The antibodies used were: Human anti-EMP3 (mouse polyclonal antibody; 1:200), ALDH1A1 (mouse polyclonal antibody; 1:200), ALDH1A3 (rabbit polyclonal antibody; 1:200), CD44 (mouse polyclonal antibody; 1:200), E-cadherin (rabbit polyclonal antibody; 1:200), N-cadherin (rabbit polyclonal antibody; 1:200), Vimentin (goat polyclonal antibody; 1:200) and TGFBR2 (rabbit polyclonal antibody; 1:200). Staining was visualized using an Alexa Fluor 488-conjugated anti-rabbit IgG antibody (cat. no. A21206; Invitrogen; Thermo Fisher Scientific, Inc.).

Nuclei were stained using DAPI (Sigma-Aldrich; Merck KGaA) for 30 min at room temperature. The stained cell samples were observed using a fluorescence microscope (Zeiss LSM510; Carl Zeiss AG; x400 magnification).

Kaplan-Meier plotter. Using the published genetic information system, Kaplan-Meier survival values were obtained (kmplot.com/analysis). This was based on results of mRNA gene chip analysis using tissues from lung cancer patients. The gene symbol used was EMP3. All conditions were set as total lung cancer patients.

Statistical analysis. All experiments were performed by repeating at least three independent experiments, and the results are expressed as the mean ± standard deviation. Each exact n value is displayed in the corresponding figure legend. To validate the data, all graphs were compared using a two-sided paired Student's t-test. $P<0.05$ was considered to indicate a statistically significant difference.

Results

EMP3 expression is increased in ALDH$^+$ NSCLC. CSCs that are resistant to cancer treatment overexpress certain proteins. Amongst these, a protein that is overexpressed together with a stem cell marker protein is classified as a CSC marker protein (32). In previous experiments, ALDH1 was used as a marker protein to classify overexpressed genes in LCSCs (33). Through classification using the feature extraction software, information on 4,300 genes that were expressed >2x higher in ALDH1$^+$ cells than in the control group was obtained (Fig. 1A). Amongst these, it was confirmed that EMP3 was highly upregulated by selecting genes associated with cell membrane proteins, and this was selected as they often serve as initiation points for signal transduction (Fig. 1B). To confirm that EMP3 was specifically overexpressed in CSCs, LCSCs were prepared by treatment with the spheroid formation assay medium, and EMP3 gene expression was increased in the LCSCs (Fig. 1C). In addition, the expression of EMP3 together with CSC marker proteins was increased in LCSCs (Fig. 1D). Based on Kaplan-Meier analysis, the prognosis of patients with high EMP3 expression amongst patients with lung cancer was significantly worse compared to those with low EMP3 expression (Fig. 1E). A total of 1,925 patients with lung cancer were included in the Kaplan-Meier analysis. Patients with low EMP3 gene expression survived an average of 81.2 months, and those with high EMP3 gene expression survived an average of 62.3 months after diagnosis. These results showed that EMP3 may be involved in the prognosis of patients with malignant lung cancer.

EMP3 promotes self-renewal and tumorigenic capacity of NSCLC. Although several studies have confirmed the functionality of the PMP22 family of proteins, little is known regarding the functionality of EMP3 in NSCLC. Therefore, in the present study, to investigate whether EMP3 was involved in the enrichment of NSCLC stem cells, A549 cells were used, an adenocarcinoma cell line that exhibits a high level of resistance to radiation and high ALDH1 expression (22). Knockdown of EMP3 expression via transfection siRNA reduced the expression of the CSC marker proteins CD133, ALDH1 and CD44. EMP3 was also overexpressed in the lung cancer cells to confirm the function of EMP3 more accurately. The cells used for overexpression were the H460 lung cancer cells, which are known to be relatively less malignant than the A549 (22). The expression levels of EMP3 in the two cells was compared (Fig. S1A). The expression of EMP3 in H460 cells was significantly lower than in A549 cells. EMP3 overexpression was thus performed using the H460 cells. The expression of CSC marker proteins was increased in the EMP3-overexpressing cells (Fig. S1B and C). Overexpression of EMP3 also reduced the expression of the CSC regulator proteins Sox2, Oct-4 and Nanog (Fig. 2A). In Fig. 2B, the difference in the expression of marker proteins according to the knockdown of EMP3 expression was confirmed using immunocytochemistry. To confirm the effect of EMP3 on CSCs, A549 cells were cultured in a serum-free medium containing epidermal growth factor and bFGF to generate spheroids. When the expression of EMP3 was suppressed using siRNA, the size and number of CSC spheres decreased significantly (Fig. 2C). Conversely, when the expression of EMP3 was overexpressed, the size and number of CSC spheres increased significantly (Fig. S1D). In addition, EMP3 is a cell membrane protein, and direct inhibitory action using an antibody was confirmed. Treatment with the anti-EMP3 antibody resulted in similar outcomes as those obtained from treatment with siRNA (Fig. 2D). A single cell assay and a limited dilution assay were performed to confirm the effects of EMP3 on self-renewal, a characteristic of CSCs. The self-renewal ability was decreased in the si-EMP3 treated group (Fig. 2E and G). As shown above, EMP3 can be directly inhibited by treatment with the anti-EMP3 antibodies. Treatment with the anti-EMP3 antibody resulted in similar outcomes as those obtained from treatment with siRNA (Fig. 2F). To assess whether EMP3 was involved in the characterization of tumor resistance to ionizing radiation, the effect of EMP3 on the clonal formation of A549 cells was investigated. Colony formation was suppressed in the EMP3 knockdown cells. These results indicate that the sensitivity to radiation was modulated by EMP3. As above, antibody treatment has a similar effect to that of EMP3 knockdown (Fig. 2H and I). CSCs have been shown to possess more than one aberration in various signaling pathways (13). Amongst them, Notch, Hedgehog (HH) and Wnt signals control stem cell self-renewal and play an important role in embryonic development and differentiation, but within CSCs, they contribute to a signaling system that promotes recurrence and metastasis of cancer by engaging in abnormal signaling. siRNA was used to confirm whether EMP3 was involved in the regulation of these important signaling systems in CSCs. The results showed that Notch, HH and Wnt signals were all regulated by EMP3 (Fig. 2J).

EMT is regulated by EMP3. Previously, a direct link has been reported between EMT progression and acquisition of stem cell properties (25,34). In general, CSC and EMT exhibit similar signaling mechanisms (35). Amongst the several features of EMT, the most distinctive is related to cancer metastasis caused by increased mobility and invasiveness of cancer cells. Cancer metastasis may be preventable by studying

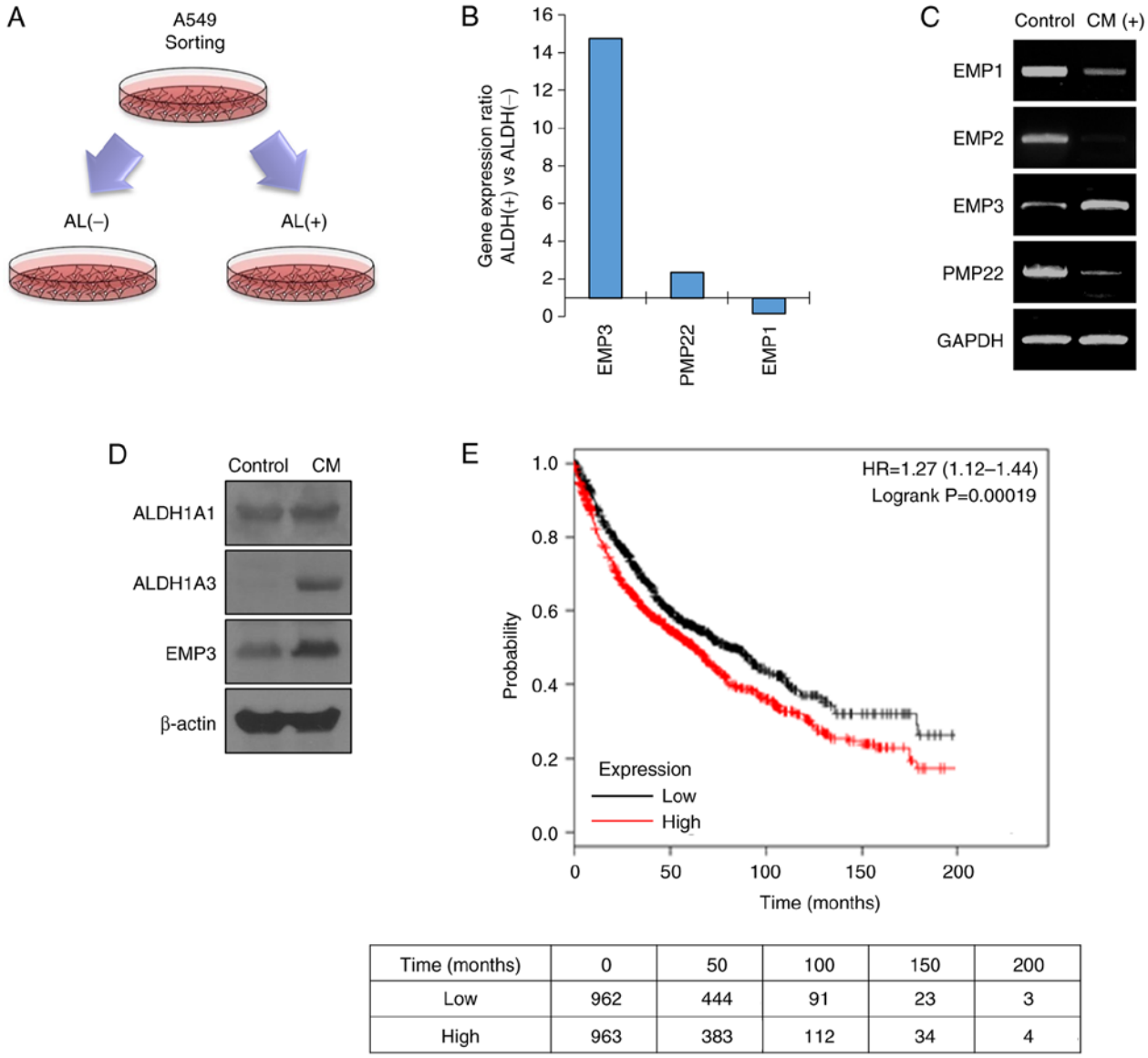

Time (months)	0	50	100	150	200
Low	962	444	91	23	3
High	963	383	112	34	4

Figure 1. EMP3 expression is upregulated in ALDH1 overexpressing A549 cells. (A) A schematic diagram of sorting of A549 cells into ALDH1^{+} and ALDH1^{-} cells using a cell sorter. (B) The expression levels of EMP family members were confirmed by microarray analysis of the gene expression levels of the sorted ALDH1$^{-/+}$ cells. Detailed information on gene expression is provided in Table SII. (C) The mRNA expression levels of the EMP family members in the A549 cells treated with CM was confirmed by PCR. GAPDH was used as a loading control. (D) Western blot analysis of CSC marker proteins ALDH1A1 and ALDH1A3. β-actin was used as a loading control. (E) Kaplan-Meier survival curve showing the survival levels of patients with lung cancer according to the expression levels of EMP3. n=1,925; log rank P=0.00019. EMP3, epithelial membrane protein 3; ALDH1, aldehyde dehydrogenase 1; PMP22, peripheral myelin protein 22-kDa; CM, conditioned media.

the signaling mechanisms associated with EMT and establishing effective control methods. However, whether EMP3 participates in EMT remains unknown, and is of interest as EMT is closely associated with CSCs. In the present study, the intracellular expression levels of E-cadherin, N-cadherin and Vimentin, which are EMT marker proteins, and Snail, slug, Twist and ZEB1, which are EMT-related transcription factors, were investigated by western blotting. When EMP3 expression was knocked down using siRNA, expression of EMT markers and EMT-related transcription factors was decreased (Fig. 3A). Immunofluorescence staining confirmed that inhibition of EMP3 expression upregulated the levels of the epithelial marker protein E-cadherin and downregulated the levels of the mesenchymal marker proteins N-cadherin and Vimentin (Fig. 3B). To confirm these results, the A549 cell line was used to evaluate the effect of EMP3 on cell migration and invasion. First, an *in vitro* wound healing assay was performed. The migration of A549 cells into the wound was significantly reduced when EMP3 gene expression was knocked down when compared with the control group (Fig. 3C). Likewise, when the A549 cell line was treated with an anti-EMP3 antibody, the migration of the cells to the wound site was significantly reduced (Fig. 3D). Conversely, when the EMP3 gene was overexpressed in the H460 cell line, cell migration into the wound was increased (Fig. S1E). Additionally, the effect of EMP3 on cell migration and cell invasion were assessed using Transwell assays. EMP3 notably regulated the invasion and migration of A549 cells (Fig. 3E and F). In the EMP3 overexpressing H460 cells, it was confirmed that cell migration and invasion was increased (Fig. S1F).

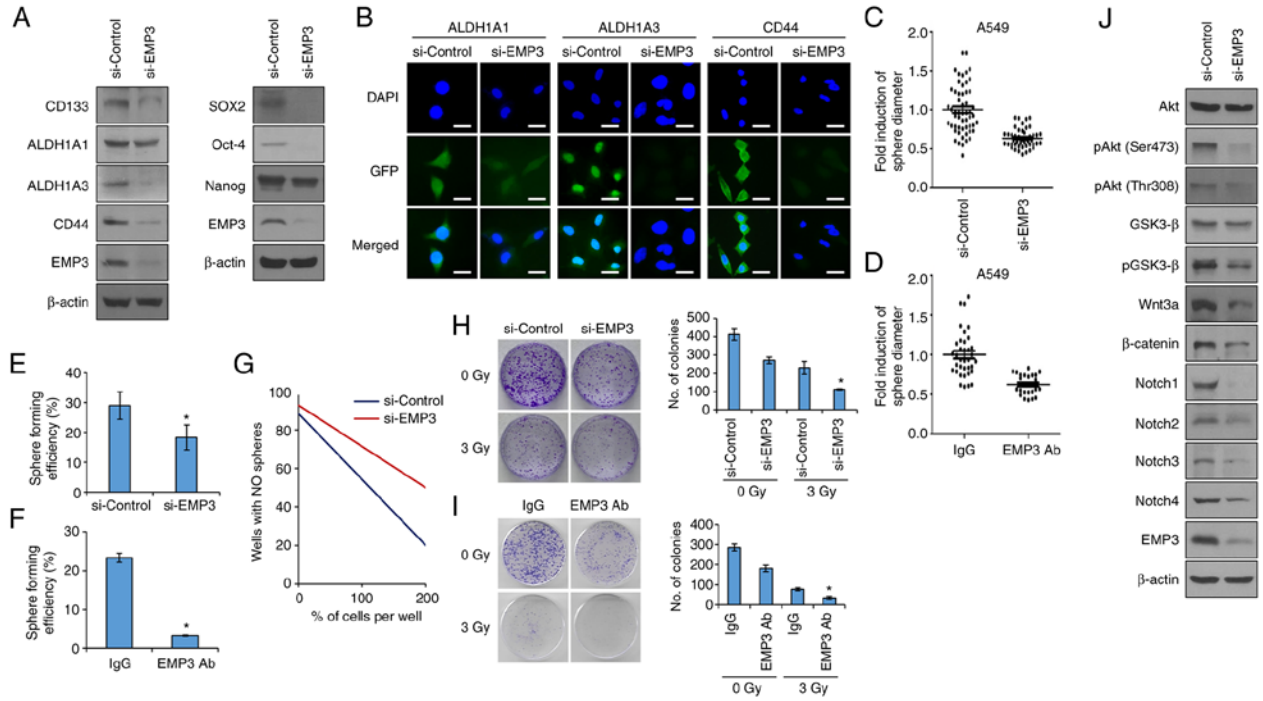

Figure 2. EMP3 regulates CSC properties in lung CSC. (A) Western blot analysis of the CSC marker proteins CD133, ALDH1A1, ALDH1A3 and CD44. The CSC regulatory proteins Sox2, Oct-4 and Nanog were also analyzed by western blotting. A549 cells were transfected with siRNA targeting EMP3. (B) Immunocytochemistry analysis of CSC marker proteins using siRNA treated A549 cells. The green signal is produced by the GFP tag on the secondary antibody. (C) Sphere-forming capacity analysis of A549 cells in siRNA transfected EMP3 cells and (D) the ability to of an anti-EMP3 antibody to abrogate sphere formation was assessed. (E) Single-cell assay of si-EMP3 transfected cells and (F) the ability of the anti-EMP3 antibody to abrogate this. (G) Limiting dilution assays were performed in 96 well plates. Wells were plated with 1, 50, 100, 150 or 200 cells/well, and conditioned media was added. Results were confirmed 10 days after seeding of cells. Colony-formation assays to observe the clonogenicity of the (H) EMP3-knockdown A549 and (I) anti-EMP3 antibody treated A549 cells. Cells were irradiated with 3 Gy radiation. After 10 days of incubation, the colonies were stained with crystal violet. (J) Western blot analysis of members of the Sonic hedgehog, Wnt/β-catenin and Notch signaling pathways in CSCs. Data are presented as the mean ± standard deviation of three repeats. Scale bar, 50 μm. *P<0.05 vs. control. EMP3, epithelial membrane protein 3; ALDH1, aldehyde dehydrogenase 1; CSC, cancer stem cell; Sox2, sex determining region Y-box 2; Oct-4, octamer-binding transcription factor 4; siRNA, small interfering RNA; p, phosphorylated; GSK3-β, glycogen synthase kinase 3-β.

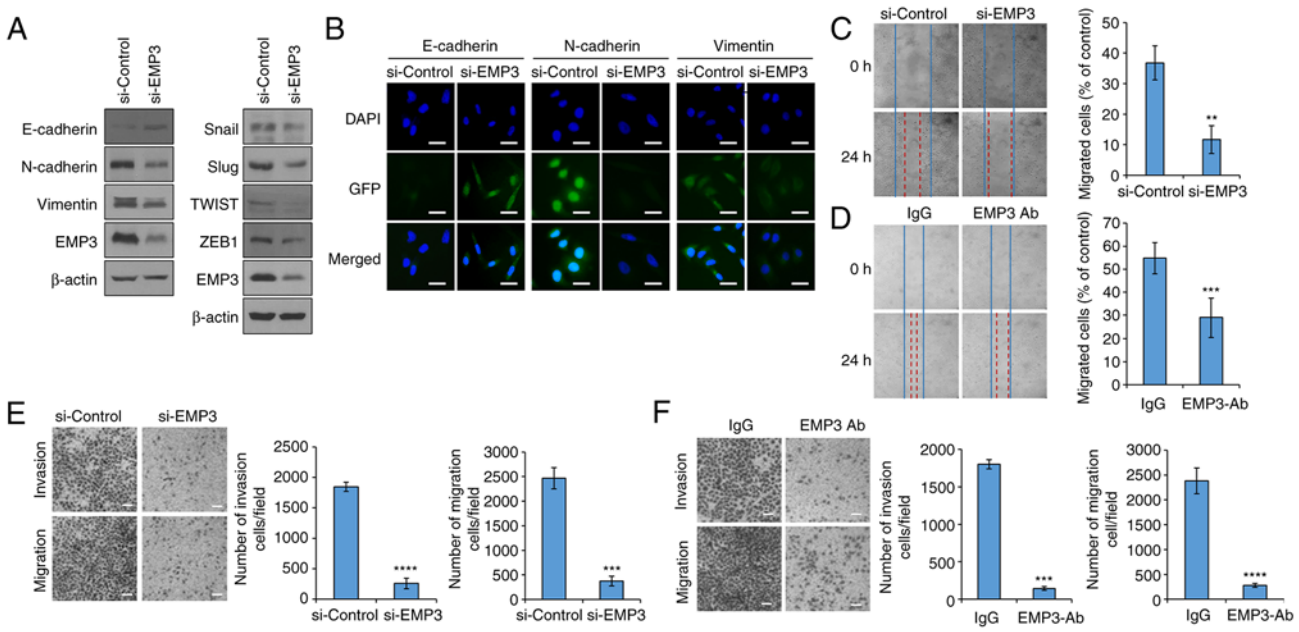

Figure 3. EMP3 is involved in EMT in lung cancer stem cells. (A) Western blot analysis of EMT marker proteins E-cadherin, N-cadherin and Vimentin. EMT regulatory proteins Snail, Slug, TWIST and ZEB1 were also analyzed by western blot. A549 cells were transfected with siRNA targeting EMP3. (B) Immunocytochemistry analysis of EMT marker proteins after transfection with siRNA targeting EMP3 in A549 cells. A primary antibody targeting each marker protein was used, and the secondary antibody used was tagged with GFP. Wound healing assays of the (C) EMP3-knockdown A549 cells and (D) anti-EMP3 antibody treated A549 cells. Migration and invasion assays of (E) EMP3-knockdown A549 cells and (F) anti-EMP3 antibody treated A549 cells. Data are presented as the mean ± standard deviation of three repeats. Scale bar, 50 μm. **P<0.01, ***P<0.001, ****P<0.0001. EMP3, epithelial membrane protein 3; EMT, epithelial-mesenchymal transition; ZEB1, Zinc finger E-box-binding homeobox 1; siRNA, small interfering RNA.

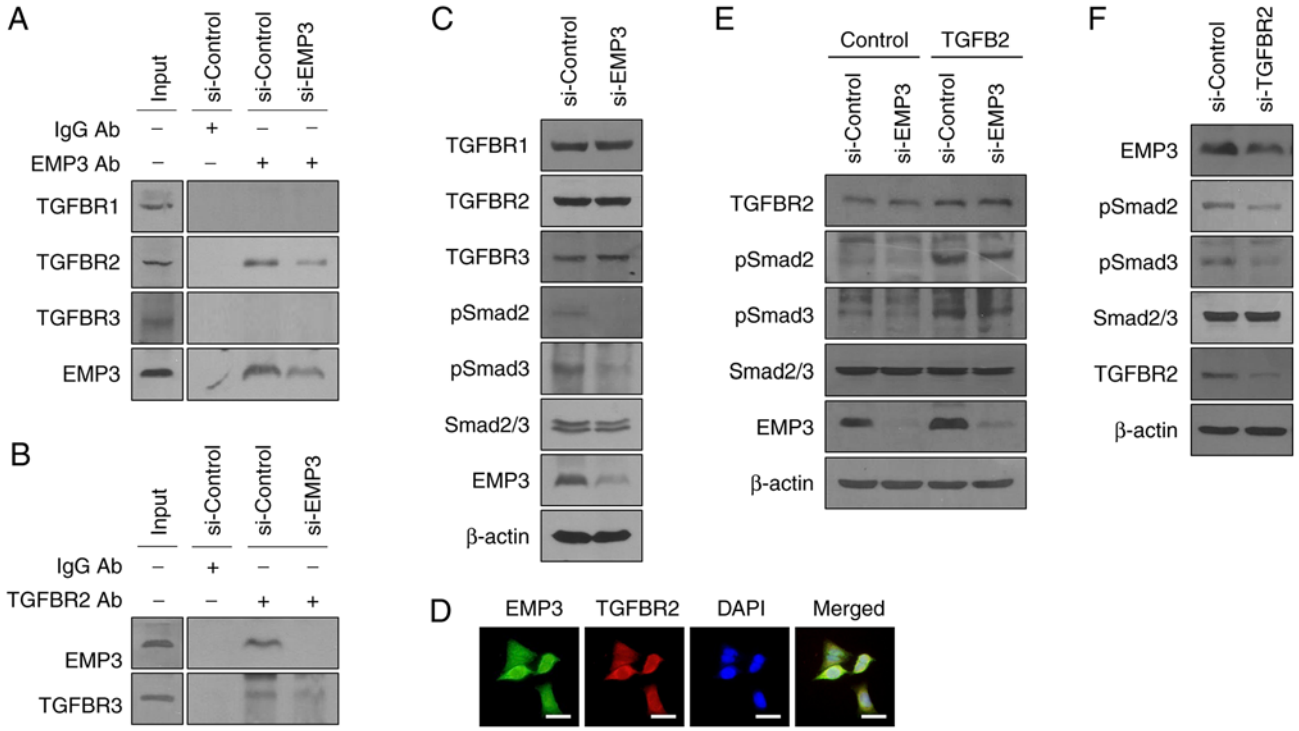

Figure 4. EMP3 regulates TGF-β signaling activation in lung cancer stem cells. (A) Immunoprecipitation analysis of EMP3 binding to TGFBRs in A549 cells. Anti-EMP3 antibodies were used to treat the EMP3-knockdown A549 lysates. (B) Immunoprecipitation analysis of TGFBR2 binding to EMP3 in A549 cells. (C) Western blot analysis of members of the TGF-β signaling pathway. β-actin was used as the loading control. (D) Immunocytochemistry analysis of the interaction between EMP3 and TGFBR2 in A549 cells. (E) After A549 cells were treated with si-EMP3, cells were treated with 20 ng/ml TGFB2 for 24 h. After treatment, cells were harvested after 48 h. (F) After treatment with si-TGFBR2, the expression of EMP3 and the TGF-β signaling members was confirmed. Scale bar, 50 μm. EMP3, epithelial membrane protein 3; TGF-β, transforming growth factor-β; TGFBR, TGF-β receptor; siRNA, small interfering RNA; p, phosphorylated.

Direct binding to TGFBR2 of EMP3 activates the downstream TGF-β/Smad signaling pathway. There are three main types of TGF-β receptors: The transmembrane serine/threonine kinase receptor, type 1 TGF-β receptor (TGFBR1), type II TGF-β receptor (TGFBR2) and β-glycan, and type III TGF-β receptor (TGFBR3) (29). IP analysis was performed to confirm the binding of three types of TGF-β receptors (TGFBR) to EMP3. EMP3 bound to TGFBR2, and this was further confirmed by IP analysis using a TGFBR2 antibody (Fig. 4A and B). In addition, western blot analysis was used to confirm the association of EMP3 with Smad downstream of TGFBR. The phosphorylation of Smad2 and Smad3 was lower in the si-EMP3 treated group, suggesting that the TGFBR-Smad signaling axis was regulated by EMP3. (Fig. 4C). Since the binding between the two proteins is related to the intracellular location, ICC analysis was used to confirm the subcellular location of EMP3 and TGFBR2, and the results showed that EMP3 and TGFBR2 were colocalized at the membrane, and that EMP3 regulated the TGFBR2-Smad signaling pathway (Fig. 4D). Additionally, following TGF-β2 (TGFB2) treatment, the sub-signaling mechanism of TGFBR was confirmed (Fig. 4E). In the cells treated with si-EMP3, it was observed that p-Smad2 and p-Smad3 levels were decreased even when treated with TGFB2. This confirmed that EMP3 was involved in the downregulation of TGFBR2 signaling through TGF-β. In addition, it was confirmed that the expression of EMP3 was lower in cells treated with si-TGFBR2 (Fig. 4F). This suggests that another mechanism linked EMP3 and TGF-β signaling.

Discussion

In the present study, it was confirmed that EMP3 expression is upregulated in LCSCs. However, according to a recent paper, EMP2, one of the EMP family proteins, has been reported to prevent cancer malignancy (36). Contrary to the increase in expression of the EMP3 gene observed in the present study, all other EMP family genes showed a decreasing trend. In LCSCs, it is necessary to confirm the change in expression and function of the other EMP family members, to compare with EMP3, and to obtain a more holistic picture of EMPs in lung cancer.

Numerous studies on the signaling process of TGFBR have been reported. Changes in TGF-β have been linked to TGFBR, and both have been associated with a variety of diseases, including cancer and inflammation (37-39). It can be confirmed that the disruption of TGF-β homeostasis occurred in samples of various several cancers (26-29). However, the specifics of the signaling processes regulated EMP3 and TGFBR2 remained to be determined, and will form the subject of future studies, and may be considered an important part of the EMP3 signaling process. In addition, TGFBR signaling has a profound relationship on the inflammatory response (37,39), and this may serve as an indication of the relationship with immune cells. CSCs inhibit the activation of immune cells and allow for evasion of immune cells, which allows for the formation of malignant cancers and metastases, and EMP3-TGFBR axis identified in the present may be involved in this process (13,40,41).

Taken together, the results confirmed that EMP3 regulates the CSC population, EMT and the phosphorylation of Smad through binding with TGFBR2. EMP3 is a protein present in the cell membrane, and can bind to various proteins present in the cell membrane, such as RTK, and integrins, as well as TGFBR2 as identified herein (42,43). In addition, it is predicted to modulate or be involved in various signaling mechanisms through binding to proteins present in cells. Furthermore, since EMP3 is present at the cell membrane, it may allow for easier targeting by drugs, a possible advantage of this protein as a potential druggable target. In general, targets present at cell membranes are easier targets for development of anticancer agents, and play an important role in regulating signals inside and outside of cells (44-46). Thus, EMP3, which is present at the cell membrane, may be an important target in the development of anticancer drugs. Furthermore, EMP3 affects sensitivity to radiation, and CSCs are characterized by resistance to ionizing radiation (13,15,22). Therefore, inhibition of EMP3 may reduce tumor resistance to ionizing radiation and maximize therapeutic efficacy. Considering these results together, it is hypothesized that EMP3 may be targeted to improve the efficacy of radiotherapy.

Acknowledgements

Not applicable.

Funding

This study was supported by a grant from the National Research Foundation of Korea (NRF) funded by the Korea government (MSIT) (grant no. NRF-2019R1C1C1009617).

Availability of data and materials

The datasets used and/or analyzed during the present study are available from the corresponding author on reasonable request.

Authors' contributions

IGK and RKK conceived and designed and the study. YJK, UJ and RKK performed the experiments. UJ and RKK performed the radiation experiments. IGK and RKK analyzed the data. IGK, YJK and RKK wrote and revised the manuscript. IGK and RKK confirm the authenticity of all the raw data.

Ethics approval and consent to participate

Not applicable.

Patient consent for publication

Not applicable.

Competing interests

The authors declare that they have no competing interests.

References

1. Ben-Porath I and Benvenisty N: Characterization of a tumor-associated gene, a member of a novel family of genes encoding membrane glycoproteins. Gene 183: 69-75, 1996.
2. Fumoto S, Hiyama K, Tanimoto K, Noguchi T, Hihara J, Hiyama E, Noguchi T and Nishiyama M: EMP3 as a tumor suppressor gene for esophageal squamous cell carcinoma. Cancer Lett 274: 25-32, 2009.
3. Alaminos M, Dávalos V, Ropero S, Setién F, Paz MF, Herranz M, Fraga MF, Mora J, Cheung NKV, Gerald WL and Esteller M: EMP3, a myelin-related gene located in the critical 19q13.3 region, is epigenetically silenced and exhibits features of a candidate tumor suppressor in glioma and neuroblastoma. Cancer Res 65: 2565-2571, 2005.
4. Xue Q, Zhou Y, Wan C, Lv L, Chen B, Cao X, Ju G, Huang Y, Ni R and Mao G: Epithelial membrane protein 3 is frequently shown as promoter methylation and functions as a tumor suppressor gene in non-small cell lung cancer. Exp Mol Pathol 95: 313-318, 2013.
5. Jun F, Hong J, Liu Q, Guo Y, Liao Y, Huang J, Wen S and Shen L: Epithelial membrane protein 3 regulates TGF-β signaling activation in CD44-high glioblastoma. Oncotarget 8: 14343-14358, 2017.
6. Hsieh YH, Hsieh SC, Lee CH, Yang SF, Cheng CW, Tang MJ, Lin CL, Lin CL and Chou RH: Targeting EMP3 suppresses proliferation and invasion of hepatocellular carcinoma cells through inactivation of PI3K/Akt pathway. Oncotarget 6: 34859-34874, 2015.
7. Hong XC, Fen YJ, Yan GC, Hong H, Yan CH, Bing LW and Zhong YH: Epithelial membrane protein 3 functions as an oncogene and is regulated by microRNA-765 in primary breast carcinoma. Mol Med Rep 12: 6445-6450, 2015.
8. Ernst A, Hofmann S, Ahmadi R, Becker N, Korshunov A, Engel F, Hartmann C, Felsberg J, Sabel M, Peterziel H, *et al*: Genomic and expression profiling of glioblastoma stem cell-like spheroid cultures identifies novel tumor-relevant genes associated with survival. Clin Cancer Res 21: 6541-6550, 2009.
9. Li JJ, Li R, Wang W, Zhang B, Song X, Zhang C, Gao Y, Liao Q, He Y, You S, *et al*: IDH2 is a novel diagnostic and prognostic serum biomarker for non-small-cell lung cancer. Mol Oncol 12: 602-610, 2018.
10. Alidousty C, Baar T, Heydt C, Wagener-Ryczek S, Kron A, Wolf J, Buettner R and Schultheis AM: Advance of theragnosis biomarkers in lung cancer: From clinical to molecular pathology and biology. J Thorac Dis 11 (Suppl 1): S3-S8, 2019.
11. Zappa C and Mousa SA: Non-small cell lung cancer: Current treatment and future advances. Transl Lung Cancer Res 5: 288-300, 2016.
12. Brognard J, Clark AS, Ni Y and Dennis PA: Akt/protein kinase B is constitutively active in non-small cell lung cancer cells and promotes cellular survival and resistance to chemotherapy and radiation. Cancer Res 61: 3986-3997, 2001.
13. Hanahan D and Weinberg RA: Hallmarks of cancer: The next generation. Cell 144: 646-674, 2011.
14. Chen SY, Huang YC, Liu SP, Tsai FJ, Shyu WC and Lin SZ: An overview of concepts for cancer stem cells. Cell Transplant 20: 113-120, 2011.
15. Rycaj K and Tang DG: Cancer stem cells and radioresistance. Int J Radiat Biol 90: 615-621, 2014.
16. Suresh R, Ali S, Ahmad A, Philip PA and Sarkar FH: The role of cancer stem cells in recurrent and drug-resistant lung cancer. Adv Exp Med Biol 890: 57-74, 2016.
17. Zhao W, Luo Y, Li B and Zhang T: Tumorigenic lung tumorospheres exhibit stem-like features with significantly increased expression of CD133 and ABCG2. Mol Med Rep 14: 2598-2606, 2016.
18. Okudela K, Woo T, Mitsui H, Tajiri M, Masuda M and Ohashi K: Expression of the potential cancer stem cell markers, CD133, CD44, ALDH1, and β-catenin, in primary lung adenocarcinoma-their prognostic significance. Pathol Int 62: 762-801, 2012.
19. Marcato P, Dean CA, Pan D, Araslanova R, Gillis M, Joshi M, Helyer L, Pan L, Leidal A, Gujar S, *et al*: Aldehyde dehydrogenase activity of breast cancer stem cells is primarily due to isoform ALDH1A3 and its expression is predictive of metastasis. Stem Cells 29: 32-45, 2011.
20. Xu SL, Liu S, Cui W, Shi Y, Liu Q, Duan JJ, Yu SC, Zhang X, Cui YH, Kung HF and Bian XW: Aldehyde dehydrogenase 1A1 circumscribes high invasive glioma cells and predicts poor prognosis. Am J Cancer Res 5: 1471-1483, 2015.

21. Vishnubalaji R, Manikandan M, Fahad M, Hamam R, Alfayez M, Kassem M, Aldahmash A and Alajez NM: Molecular profiling of ALDH1$^+$ colorectal cancer stem cells reveals preferential activation of MAPK, FAK, and oxidative stress pro-survival signalling pathways. Oncotarget 9: 13551-13564, 2018.
22. Kim IG, Kim SY, Choi SI, Lee JH, Kim KC and Cho EW: Fibulin-3-mediated inhibition of epithelial-to-mesenchymal transition and self-renewal of ALDH$^+$ lung cancer stem cells through IGF1R signaling. Oncogene 33: 3908-3917, 2014.
23. Buck E, Eyzaguirre A, Barr S, Thompson S, Sennello R, Young D, Iwata KK, Gibson NW, Cagnoni P and Haley JD: Loss of homotypic cell adhesion by epithelial-mesenchymal transition or mutation limits sensitivity to epidermal growth factor receptor inhibition. Mol Cancer Ther 6: 532-541, 2007.
24. Creighton CJ, Li X, Landis M, Dixon JM, Neumeister VM, Sjolund A, Rimm DL, Wong H, Rodriguez A, Herschkowitz JI, *et al*: Residual breast cancers after conventional therapy display mesenchymal as well as tumor-initiating features. Proc Natl Acad Sci USA 106: 13820-13825, 2009.
25. Singh A and Settleman J: EMT, cancer stem cells and drug resistance: An emerging axis of evil in the war on cancer. Oncogene 29: 4741-4751, 2010.
26. Du S, Bouquet S, Lo CH, Pellicciotta I, Bolourchi S, Parry R and Barcellos-Hoff MH: Attenuation of the DNA damage response by transforming growth factor-beta inhibitors enhances radiation sensitivity of non-small-cell lung cancer cells in vitro and in vivo. Int J Radiat Oncol Biol Phys 91: 91-99, 2015.
27. Murai F, Koinuma D, Shinozaki-Ushiku A, Fukayama M, Miyaozono K and Ehata S: EZH2 promotes progression of small cell lung cancer by suppressing the TGF-β-Smad-ASCL1 pathway. Cell Discov 1: 15026, 2015.
28. Xu J, Lamouille S and Derynck R: TGF-beta-induced epithelial to mesenchymal transition. Cell Res 19: 156-172, 2009.
29. Hao Y, Baker D and Dijke PT: TGF-β-mediated epithelial-mesenchymal transition and cancer metastasis. Int J Mol Sci 20: 2767, 2019.
30. Wang Y and Shang Y: Epigenetic control of epithelial-to-mesenchymal transition and cancer metastasis. Exp Cell Res 319: 160-169, 2013.
31. Palma Cde S, Grassi ML, Thomé CH, Ferreira GA, Albuquerque D, Pinto MT, Melo FU, Kashima S, Covas DT, Pitteri SJ and Faça VM: Proteomic analysis of epithelial to mesenchymal transition (EMT) reveals cross-talk between SNAIL and HDAC1 proteins in breast cancer cells. Mol Cell Proteomics 15: 906-917, 2016.
32. Takahashi K and Yamanaka S: Induction of pluripotent stem cells from mouse embryonic and adult fibroblast cultures by defined factors. Cell 126: 663-676, 2006.
33. Choi SI, Lee JH, Kim RK, Jung U, Kahm YJ, Cho EW and Kim IG: HSPA1L enhances cancer stem cell-like properties by activating IGF1Rβ and regulating β-catenin transcription. Int J Mol Sci 21: 6957, 2020.
34. Mani SA, Guo W, Liao MJ, Eaton EN, Ayyanan A, Zhou AY, Brooks M, Reinhard F, Zhang CC, Shipitsin M, *et al*: The epithelial-mesenchymal transition generates cells with properties of stem cells. Cell 133: 704-715, 2008.
35. Morel AP, Lièvre M, Thomas C, Hinkal G, Ansieau S and Puisieux A: Generation of breast cancer stem cells through epithelial-mesenchymal transition. PLoS One 3: e2888, 2008.
36. Ma Y, Schröder DC, Nenkov M, Rizwan MN, Abubrig M, Sonnemann J, Murrieta-Coxca JM, Morales-Prieto DM, Westermann M, Gassler N and Chen Y: Epithelial membrane protein 2 suppresses non-small cell lung cancer cell growth by inhibition of MAPK pathway. Int J Mol Sci 22: 2944, 2021.
37. Blobe GC, Schiemann WP and Lodish HF: Role of transforming growth factor beta in human disease. N Engl J Med 342: 1350-1358, 2000.
38. de Caestecker MP, Piek E and Roberts AB: Role of transforming growth factor-beta signaling in cancer. J Natl Cancer Inst 92: 1388-1402, 2000.
39. Yoshinaga K, Obata H, Jurukovski V, Mazzieri R, Chen Y, Zilberberg L, Huso D, Melamed J, Prijatelj P, Todorovic V, *et al*: Perturbation of transforming growth factor (TGF)-beta1 association with latent TGF-beta binding protein yields inflammation and tumors. Proc Natl Acad Sci USA 105: 18758-18763, 2008.
40. Korkaya H, Liu S and Wicha MS: Regulation of cancer stem cells by cytokine networks: Attacking cancer's inflammatory roots. Clin Cancer Res 17: 6125-6129, 2011.
41. Zhou C, Liu J, Tang Y and Liang X: Inflammation linking EMT and cancer stem cells. Oral Oncol 48: 1068-1075, 2012.
42. Christians A, Poisel E, Hartmann C, Deimling AV and Pusch S: Characterization of the epithelial membrane protein 3 interaction network reveals a potential functional link to mitogenic signal transduction regulation. Int J Cancer 145: 461-473, 2019.
43. Wang YW, Li WM, Wu WJ, Chai CY, Liu HS, Lai MD and Chow NH: Potential significance of EMP3 in patients with upper urinary tract urothelial carcinoma: Crosstalk with ErbB2-PI3K-Akt pathway. J Urol 192: 242-251, 2014.
44. Lin CY, Lee CH, Chuang YH, Lee JY, Chiu YY, Lee YH, Jong YJ, Hwang JK, Huang SH, Chen LC, *et al*: Membrane protein-regulated networks across human cancers. Nat Commun 10: 3131, 2019.
45. Pasto A, Giordano F, Evangelopoulos M, Amadori A and Tasiotti E: Cell membrane protein functionalization of nanoparticles as a new tumor-targeting strategy. Clin Transl Med 8: 8, 2019.
46. Schmit K and Michiels C: TMEM proteins in cancer: A review. Front Pharmacol 9: 1345, 2018.